American Journal of Materials Science 2015, 5(3A): 39-47
DOI: 10.5923/s.materials.201502.07

High Energy Radiation Effects on the Seebeck Coefficient, van der Pauw-Hall Effect Parameters and Optical Properties of Si/Si+Sb Multi-Nanolayered Thin Films

S. Budak[1,*], E. Gulduren[2], B. Allen[1], J. Cole[1], J. Lassiter[3], T. Colon[4], C. Muntele[5], R. Parker[6], C. Smith[7], R. B. Johnson[1,4]

[1]Department of Electrical Engineering & Computer Science, Alabama A&M University, Normal, AL USA
[2]Department of Physics, University of Alabama in Huntsville, Huntsville, AL USA
[3]Materials Research Laboratory, Alabama A&M University, Normal, AL USA
[4]Department of Physics, Chemistry, and Mathematics, Alabama A&M University, Normal, AL USA
[5]Cygnus Scientific Services, Huntsville, AL USA
[6]Marshall Flight and Space Center, Huntsville, AL USA
[7]4 SIGHT INC. Huntsville, AL USA

Abstract We have prepared thermoelectric devices from alternating layers of Si/Si+Sb superlattice films using the electron beam deposition (EBD). In order to determine the stoichiometry of the elements and the thickness of the grown multi-layer film, Rutherford Backscattering Spectrometry (RBS) and RUMP simulation have been used. The 5 MeV Si ions bombardments have been performed using the AAMU Pelletron ion beam accelerator, to form quantum clusters in the multi-layer superlattice thin films to improve the thermoelectric and optical properties for more efficient thermoelectric devices. The fabricated multilayered thermoelectric devices have been characterized using cross plane electrical conductivity and Seebeck coefficient, van der Pauw resistivity, density, mobility, Hall coefficient, optical absorption, photoluminescence (PL), Raman, and AFM measurements. High-energy ion beam modification caused some remarkable thermoelectric and optical properties.

Keywords Ion bombardment, Seebeck coefficient, Multi-Nanolayers, Figure of merit, van der Pauw resistivity, Hall Effect

1. Introduction

The use of waste heat from mobile and stationary energy conversion processes to optimize power generation (cars: substitution of the alternator; power plants and combined heat and power production: power production plus), and also to optimize combustion in simple wood stoves (electric-driven fans for air supply) is considered promising fields of application [1]. Thermoelectric generators (TEG) can convert waste heat into electric energy without using moving parts and without producing carbon dioxide gas, toxic substances or other emissions. It is expected that thermoelectric power generation can provide a new energy source from the conversion of waste heat emitted by automobiles, factories, and other similar sources [2]. Earlier studies of thermoelectric materials and their applications were based on bulk materials. However, with the increasing combination of a higher heat flux with a higher package density in microelectronic devices, it is becoming more challenging to provide sufficient heat dissipation from the package. Therefore, thin film thermoelectric devices with an efficient cooling capacity, small area, and short response time are in high demand. The efficiency per unit area of thermoelectric devices made of thin films is higher than that of devices made of bulk materials, and thin film thermoelectric devices can be applied in more diverse fields [3]. In general, a TEG consists of a number of semiconductor pairs that are connected electrically in series and thermally in parallel, and each pair includes a p-type and an n-type element. Although in theory, a single piece of semiconductor material could work, a series connection is used to meet the high voltage potential requirements. P-type and n-type elements are alternated to assure that the carriers transport in the same direction [4]. In most of the power generation applications, the figure of merit is on the order of 1 resulting in low device thermal efficiency. Although the research into thermoelectric material development for high figure of merit is progressing, the maximum device thermal efficiency is still on the order of less than 10% [5]. In order to improve the

* Corresponding author:
satilmis.budak@aamu.edu (S. Budak)
Published online at http://journal.sapub.org/materials

thermoelectric properties of thermoelectric materials, thin film technique is used due to the stronger quantum confinement compared to that of their bulk materials [6]. A combination of recent significant advances in the scientific understanding of quantum wells, nanostructure effects on thermoelectric (TE) properties, and modern thin-layer and nano-scale manufacturing technologies have produced the advanced TE materials with potential conversion efficiencies of over 15%. The advent of these advanced TE materials offers new opportunities to recover waste heat more efficiently and economically with highly reliable and relatively passive systems that eliminate noise and vibration. A TEG device produces voltage when a temperature difference (DT) occurs between the two sides of the device because of the thermoelectric effect [7]. With the help of the technology of quantum-well super-lattices, quantum-dot super-lattices, nano-tubes, etc., nano-structured thermoelectric devices could provide the possibility of substantially increasing the thermoelectric figure of merit. It may be expected that micro-/nano-scaled heat engines will be one of the important applications in nano-technology in the near future [8]. Many interdisciplinary areas like physics, chemistry, and material sciences are developing so rapidly. Ion induced modifications of solids, thin films, surface and interfaces are such fields emerged as areas to quantify the properties of solids up to a shallow depth [9]. The efficiency of the thermoelectric materials and devices, the figure of merit is defined by $ZT = S^2\sigma T / \kappa$, where S is the Seebeck coefficient, σ is the electrical conductivity, T is the absolute temperature, and κ is the thermal conductivity. ZT could be increased by increasing S, by increasing σ, or by decreasing κ. In order to compete with conventional refrigerators, a ZT of 3 is required. Due to their limited energy conversion efficiencies (i.e. ZT is ~ 1); thermoelectric devices currently have a rather narrow set of applications [10, 11]. Some of the previous works [12-16] focused on Si-Ge thin film systems, which were either SiGe single layered thin film, Si/Si+Ge multilayered superlattice thin film or (because of the preceding 'either') Si/Ge multilayered thin film systems. We have reached remarkable thermoelectrical and optical properties from those studies. These results and some of our Sb results from our other studies encouraged us to work on Si/Si+Sb multilayered thin film systems. In this study, we reported the growth of Si/Si+Sb multilayer superlattice films using the electron beam deposition (EBD) and performed thermoelectrical and optical characterizations. The produced thin films were bombarded with high-energy Si ions for increasing cross plane electrical conductivity, decreasing van der Pauw resistivity, and tailoring carrier density, mobility, and Hall coefficient. In addition to those measurements, we have also performed some optical characterizations like optical absorption, photoluminescence (PL), Raman, and Atomic Force Microscopy (AFM) measurements. *We will be continuing the in-plane and cross-plane thermal conductivity measurements in our future studies with our new Laser PIT thermal conductivity and 3w thermal conductivity measurement systems.*

2. Experimental

We have deposited the Si/Si + Sb multi-nano-layered films on silicon and silica (suprasil) substrates using the electron beam deposition (EBD). Silica (suprasil) substrate is used for optical absorption, photoluminescence and Seebeck coefficient measurements, 100 nm oxidized Si substrates are used for the electrical conductivity measurements, Raman, and AFM measurements. Multilayer thin film systems have been prepared as 20 or 50 multilayered structures. 20 and 50 multilayers were sequentially deposited to have 10 and 25 periodic structures consisting of alternating Si and Si + Sb layers. The base pressure obtained in the chamber was about $3x10^{-6}$ Torr. A gold-coated INFICON quartz crystal microbalance (QCM) monitor was used to monitor the growth rate during the multilayer deposition. The film geometries used for deposition of Si/Si + Sb multi-nano-layers to apply the cross plane electrical and optical measurements are shown in Fig. 1. Pelletron ion beam accelerator at the Alabama A&M University, Materials Research Laboratory (AAMU-MRL) was used to bombard the multi-nano-layered Si/Si+Sb thin films at the energies of 2 and 5 MeV for 20 and 50 multilayers to form nano-dots and /or nano-clusters to increase the electrical conductivity and Seebeck coefficients, and change the optical properties. In this study, we do not have the thermal conductivity measurements.

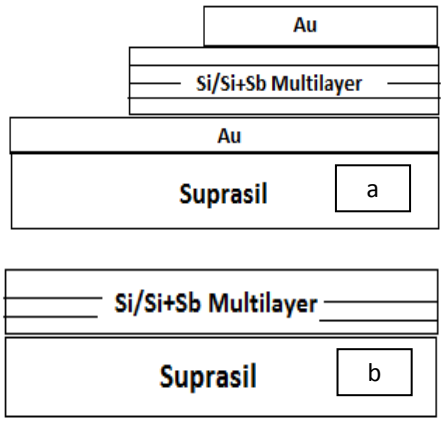

Figure 1. Geometry (a) for the cross plane Seebeck coefficient and electrical conductivity, (b) for van der Pauw-Hall Effect measurements and for the optical absorption and photoluminescence measurements

The fabricated multilayered thermoelectric devices have been characterized using cross-plane electrical conductivity and Seebeck coefficient, van der Pauw resistivity, density, mobility, Hall coefficient, optical absorption, and photoluminescence, Raman, and AFM measurements. The energy of the bombarding Si ions was chosen by the SRIM simulation software. The fluences used for the bombardment were between $1x10^{12} ions/cm^2$ and $1x10^{14} ions/cm^2$. Rutherford Backscattering Spectrometry (RBS) was performed using 2.1 MeV He^+ ions with particle detector placed at 170° from the incident beam to monitor the elemental analysis [17-19]. The optical absorption spectra of

films were recorded in the range 200 – 800 nm with a CARY 5000 UV–Vis–NIR spectrophotometer. The photoluminescence (PL) measurements were performed on a CARY Eclipse Spectrometer at an excitation wavelength of 350 nm.

3. Results and Discussion

Figure 2 shows the cross plane electrical conductivity measurements for 20 alternating layers of Si/Si + Sb multi-nano-layered thin films depending on the applied 2 MeV Si ions bombardment fluences. As seen from the figure 2, the electrical conductivity started to decrease when the first ion bombardment fluence of $1x10^{12} ions/cm^2$ was introduced and then the electrical conductivity increased until the fluence of $5x10^{13} ions/cm^2$. After the fluence of $5x10^{13} ions/cm^2$, the electrical conductivity decreased again. First decrease in the electrical conductivity could arise from the thermal stabilization after the high-energy beam was introduced. After the thermal stabilization, the increase in the charge carrier concentration could cause an increase in the electrical conductivity. Applied high-energy beam did not affect too much the cross plane electrical conductivity in the increasing direction. High electrical conductivity is one of the desired things for the high efficient thermoelectric devices and materials. Si ions bombardment could increase the charge carrier concentration and could cause an increase in the electrical conductivity.

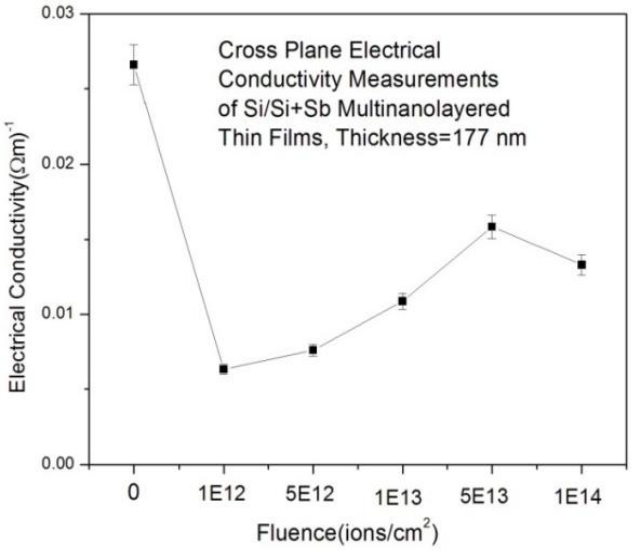

Figure 2. Fluence dependence of the cross- plane electrical conductivity of 20 alternating layers of Si/Si+Sb thin films

We have seen the increase between the fluences of $1x10^{12} ions/cm^2$ and $5x10^{13} ions/cm^2$. This interval might be good for this film system. Forming nano-structuring could cause higher electrical conductivity [20].

Figure 3 shows the fluence dependence of optical absorption spectra of 20 alternating layers of Si/Si+Sb thin films. As seen from the figure 3, the optical absorption spectra look like each other except for the shifting in y-direction. But the relative amplitudes as a function of wavelength almost stay unchanged. There are three absorption peaks that appeared at 350, 550, and 640 nm from the 20 alternating Si/Si+Sb multilayer thin films. These absorption peaks were labeled on the figure 3. Zhong et al. (2014) found the optical absorption peak for Sb at 566 nm. What we got at 550 nm and 640 nm could come from Sb nanoparticles in the thin film system [21]. Eckhoff et al. (2005) showed the optical absorption from the Si nano-particles at about 280 nm. Our peak in the graph at 350 nm could come from Si nanoparticles from the multilayer thin film [22].

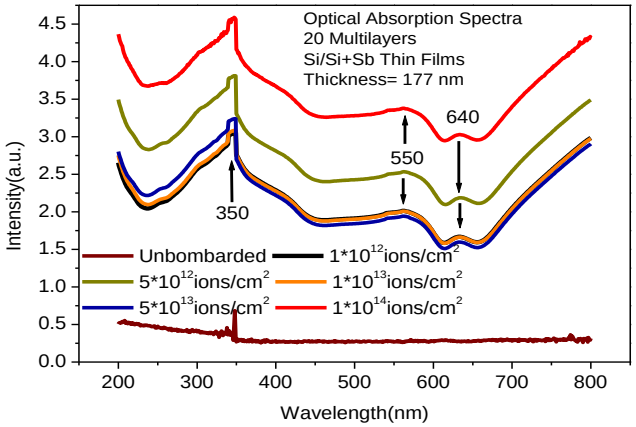

Figure 3. Fluence dependence of optical absorption spectra of 20 alternating layers of Si/Si+Sb thin films

Figure 4 shows the fluence dependence of PL spectra of 20 alternating layers of Si/Si+Sb thin films. Ion beam bombardment caused a positive effect in the PL spectra. There are three peaks at about 480, 525, and 550 nm. These peaks were labeled on the figure 4. The highest peaks were recorded at 550 nm. When the ion beam bombardment fluence increases, the intensity of the peaks gets sharper and bigger except for the fluence of $1x10^{14}$ ions/cm^2 even though the fluence of $1x10^{14}$ ions/cm^2 is the highest one.

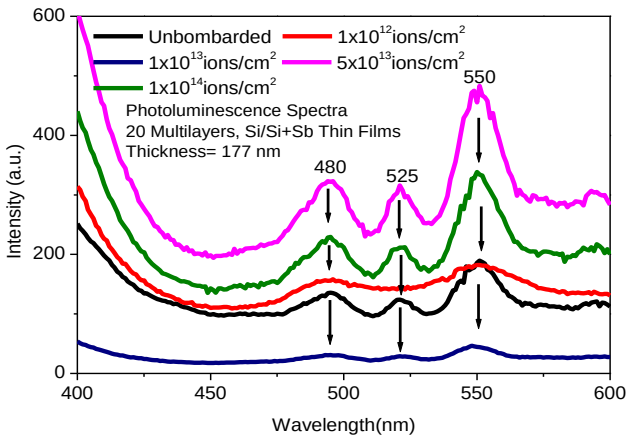

Figure 4. Fluence dependence of photoluminescence spectra of 20 alternating layers of Si/Si+Sb thin films

The reason why we could not get the highest peak at the

highest fluence might be the damage of the thin film structures at this fluence. The reason of higher peaks at higher fluences might be coming from the Sb nano-dots and / or nano-clustering formation in the multilayers. Ma et al. has studied and showed the PL spectra from Si nano-particles at about 475, 550, and 725 nm [23]. It seems that the signal comes from Sb element and combines with the peak of Si element during the deposition of alloy thin films of Si/Si+Sb. Many literature studies show that people are using Sb atoms with some other elements like ZnO for nanowire, optical properties. Doping percentage of Sb into the other materials shifts the place of the peak, and by this way the optical properties of the doped materials tailor for the special purposes. One literature study is given as an example [24].

Figure 5 shows RBS and RUMP graphs of 50 alternating layers of Si/Si+Sb thin films. After we studied the 20 multilayers of Si/Si+Sb thin film systems, we decided to continue with the more multilayers and much thicker forms of Si/Si+Sb thin film systems since we had more promising properties from the electrical conductivity, optical absorption, and photoluminescence spectroscopies. Thus, we increased the number of the layers and the thickness of the samples by 2.5 times. Then we reached the 50 alternating Si/Si+Sb multilayer thin film systems at the thickness of 430 nm for more remarkable research on the thermoelectrical and optical properties. The black dots show the experimental results of RBS spectrum, and continuous black curve shows the fitted RUMP simulation on the RBS experimental data. As seen from the figure 5, the RUMP simulation curve fits quite well on the experimental RBS data. During RUMP simulation the Si and Sb amount were inserted at different amounts until the simulation comes up quite well with the experimental RBS data while we were using layered thin film structures. Those information were shown as "layer, thickness and composition" in the figure. The thickness shown in the figure is in the atomic layer thickness. Then, we converted the atomic layer thickness to the real thin film thickness by using some conversion relation, and we calculated the thickness of the thin film.

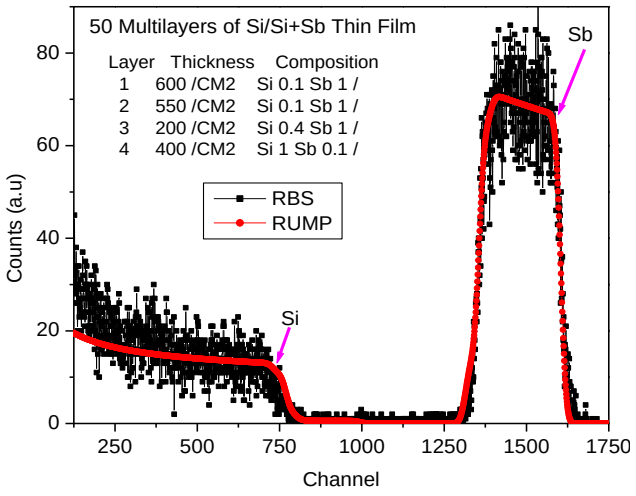

Figure 5. RBS and RUMP graphs of 50 alternating layers of Si/Si+Sb thin films

Figure 6 shows the fluence dependence of the cross-plane Seebeck coefficient of 50 alternating layers of Si/Si+Sb thin films (a) at different temperatures, (b) at room temperature. Ion beam bombardment caused some positive effects on the Seebeck coefficient at the suitable fluences under the temperature variation. The increase in the Seebeck coefficients is one of the expected outcomes for the high efficient thermoelectric devices and material systems. Some high-energy fluences did not affect the thermoelectric thin film systems in the increasing direction of Seebeck coefficient. As seen from figure 6b, the increase in the high ion beam fluences at the room temperature caused increase in Seebeck coefficient in negative direction. More charge carrier concentration due to high-energy Si ion implantation caused higher Seebeck values. After the fluence of $7x10^{12} ions/cm^2$, the Seebeck value started to decrease. Depending on the material systems, the high energy ions beam bombardment might have an effect to increase the Seebeck coefficients since the ion beam bombardment could increase the charge carrier concentration in the thin film systems. Even the Seebeck coefficient increases in *negative* direction due to the type of materials like n-type and p-type semiconductors, the figure of merit increases due to the square of the Seebeck coefficient in the figure of merit equation.

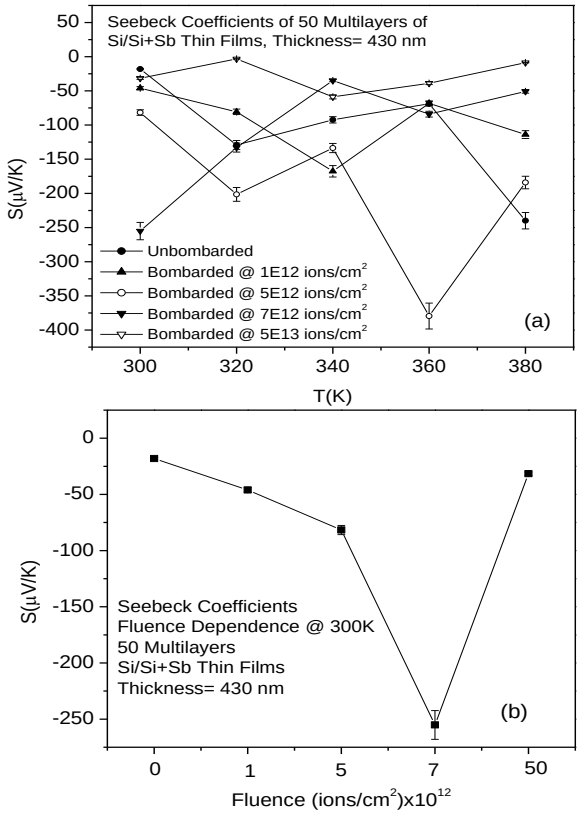

Figure 6. Fluence dependence of the cross- plane Seebeck coefficient of 50 alternating layers of Si/Si+Sb thin films (a) at the different temperatures, (b) at room temperature

Figure 7 shows the fluence dependence of the van der Pauw resistivity measurements of 50 alternating layers of Si/Si+Sb thin films at the different temperatures. The van der Pauw resistivity values were affected from the ion beam bombardment in positive directions even there are decrements and increments depending on the temperature variations as seen in figure 7. If one could look at the y-axis and values of the van der Pauw resistivity values, the magnitudes of the resistivity values decreased depending on the increased values of the applied fluences. The decrease in resistivity means an increase in the electrical conductivity. The higher electrical conductivity values are necessary for the high efficient thermoelectric materials and devices.

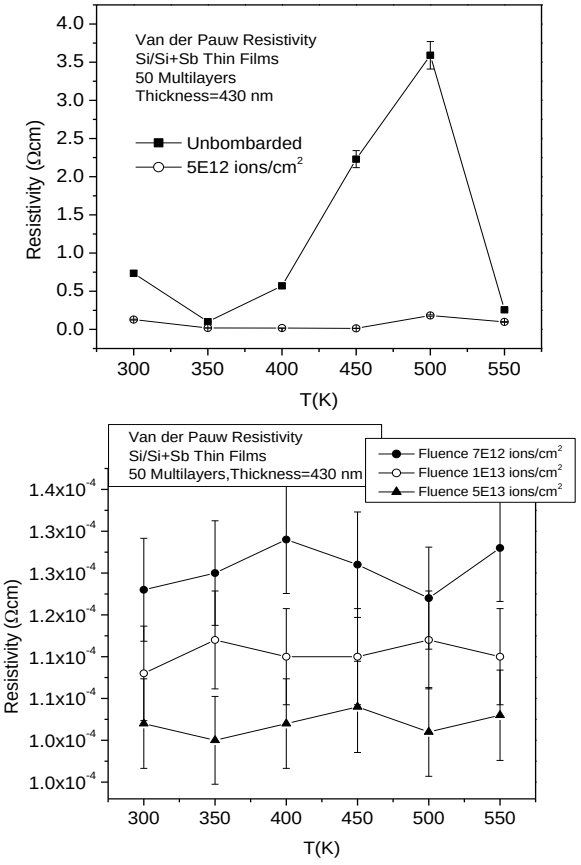

Figure 7. Fluence dependence of the van der Pauw resistivity measurements of 50 alternating layers of Si/Si+Sb thin films at the different temperatures

Figure 8 shows the fluence dependence of the van der Pauw resistivity measurements of 50 alternating layers of Si/Si+Sb thin films at the room temperature. The decrease in the resistivity with the increasing ion beam fluence could be seen more clearly in figure 8. Figure 8 explains the positive effects of the ion beam bombardment on the electrical resistivity values since the electrical resistivity values decreased while the high energy ion beam fluence increased. Decrease in the electrical resistivity means increase in the electrical conductivity.

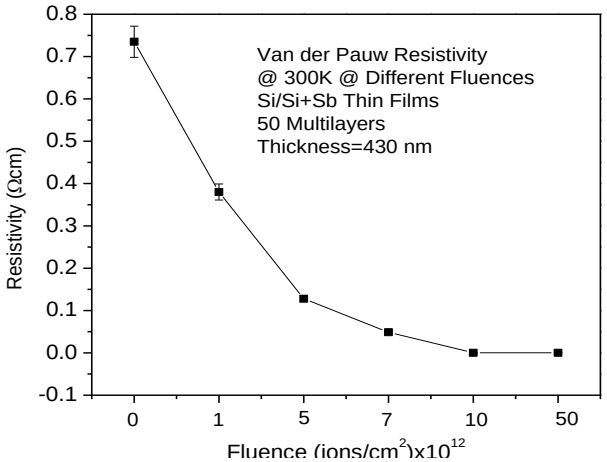

Figure 8. Fluence dependence of the van der Pauw resistivity measurements of 50 alternating layers of Si/Si+Sb thin films at the room temperature

The increase in the electrical conductivity is another expected parameter for the high efficient thermoelectric devices and materials.

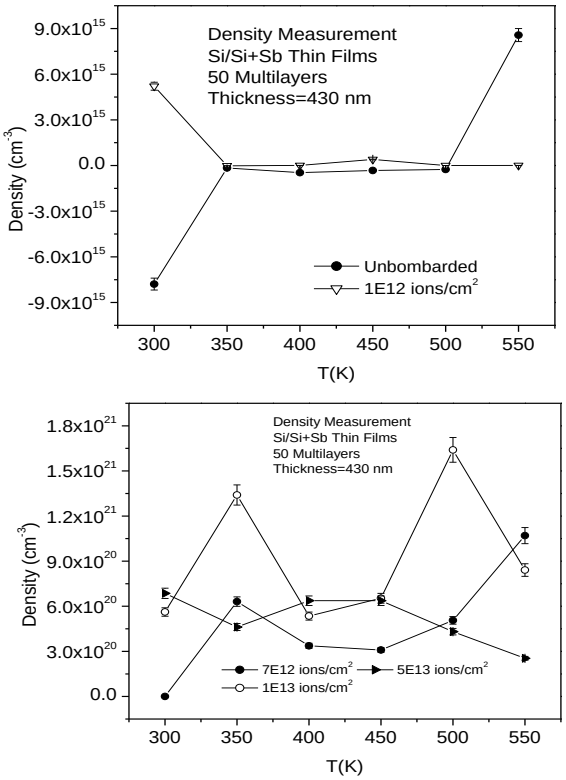

Figure 9. Fluence dependence of the density measurements of 50 alternating layers of Si/Si+Sb thin films at the different temperatures

Figure 9 shows the fluence dependence of the density measurements of 50 alternating layers of Si/Si+Sb thin films at the different temperatures. The density values shifted from negative direction to the positive direction while the ion bombardment fluences were increasing as if the multilayer

thin film systems behave like moving from n-type structures to p-type structures. This might be due to the 5 MeV Si ions bombardments on the 50 multilayer Si/Si+Sb thin film systems. As seen from the figure 9, when the ion beam fluence increased, the density values reached higher values due to increase in charge carrier concentration in the thin film system. Depending on the charge doping due to ion bombardment, the multilayer thin film systems could behave like a material system as if the type of the material systems might change depending on the dominant charge carrier concentrations like electrons and holes.

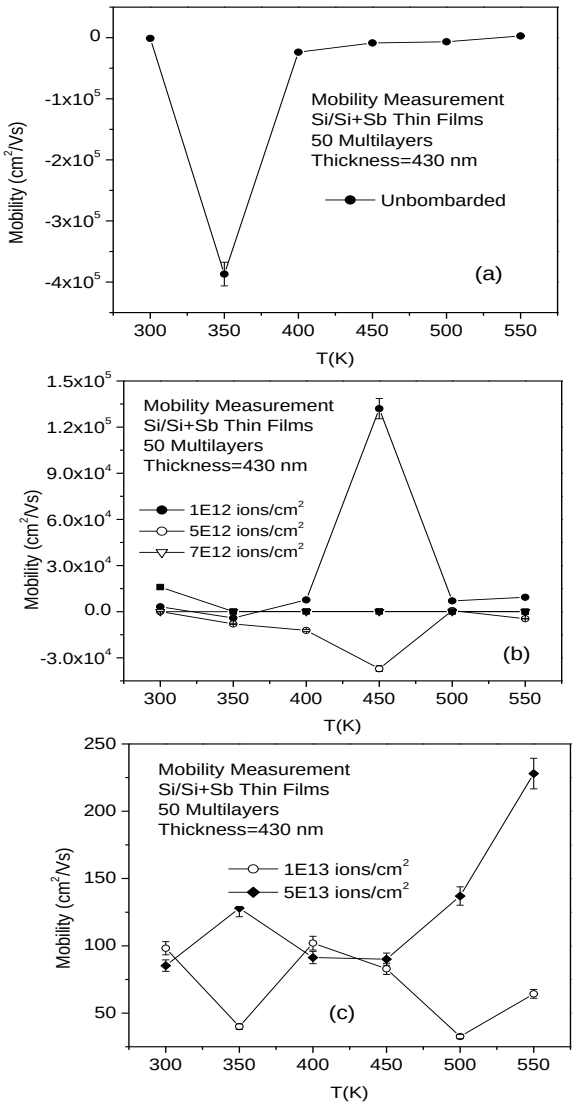

Figure 10. Fluence dependence of the mobility measurements of 50 alternating layers of Si/Si+Sb thin films at the different temperatures

Figure 10 shows the fluence dependence of the mobility measurements of 50 alternating layers of Si/Si+Sb thin films at the different temperatures. Similar effects like in density behavior, the mobility measurements shift from negative behavior side to positive behavior side like from n-type structures to the p-type structures at the suitable fluences even though there are fluctuations like increasing and decreasing depending on the increase of the temperatures. As seen from the figure 10 a through c, the magnitude of the mobility values decreased while the ion beam fluence increased. That could be expected since high fluence means that more amounts of the ions have been bombarded and inserted through thin film systems per unit area. The more charge (particles) in the unit area, the less mobility among the particles. More gathering of the charged particle could increase the electrical conductivity since the number of the charged particles could increase in the unit area.

Figure 11 shows the fluence dependence of the Hall coefficient measurements of 50 alternating layers of Si/Si+Sb thin films at the different temperatures. We have seen the similar effects in Hall coefficients like in mobility and density measurements. While the high energy beam bombardment was being continued at the higher fluences, the Hall coefficients shifted from n-type structures to p-type structures. The reason could arise from the modification of the thin film systems by high charge concentrations. While the fluences increased, the magnitude of the Hall coefficients decreased due to the doping Si, which changes the multilayer structures and the balance of the charge distributions in the thin film system.

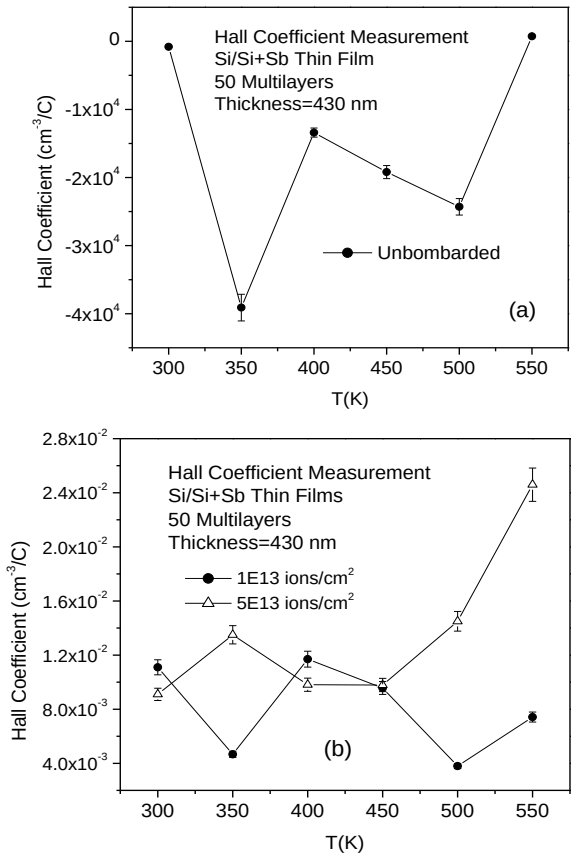

Figure 11. Fluence dependence of the Hall coefficient measurements of 50 alternating layers of Si/Si+Sb thin films at the different temperatures

Figure 12 shows the Raman Spectra of 50 alternating Si/Si+Sb multilayer thin films: a) Unannealed and b) annealed at 100℃. As seen from the figure 12, the Sb peak decreased when it was annealed at 100℃ since some amount of Sb on the surface might diffuse in the multilayer structures due to temperature annealing. *In future studies related to the similar thin film structures, we are planning to conduct more detailed Raman spectroscopy studies at the different annealing temperatures to see the effects of the annealing on Sb element on the surface and in the multilayer structures.*

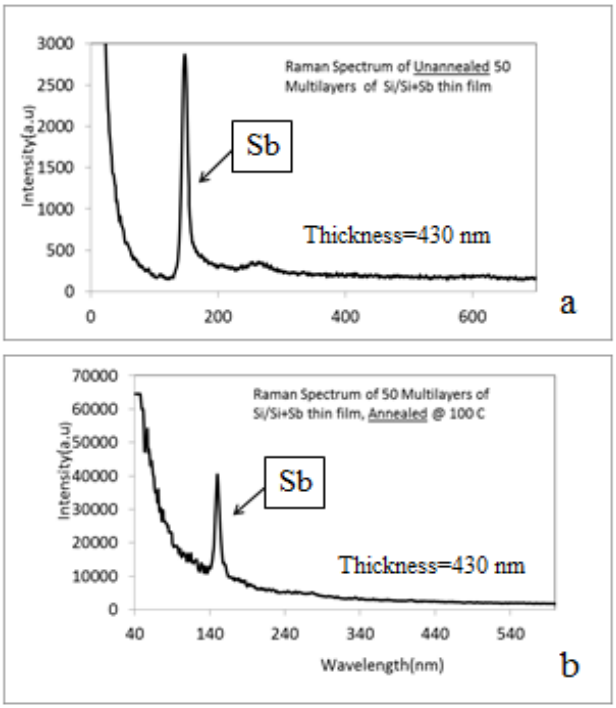

Figure 12. Raman spectra of 50 alternating Si/Si+Sb multilayer thin films: a) Unannealed and b) annealed at 100℃

Figure 13 shows the photoluminescence (PL) spectra of 50 alternating Si/Si+Sb multilayer thin films: a) Unannealed and b) annealed at 100℃. Peaks get sharper and become a little bit bigger when the thin film structure was annealed at 100℃. *According to the plan we mentioned for Raman spectroscopy, we are planning more detailed PL studies on the similar thin film systems for reaching higher efficient thermoelectric material systems using the optimized values.*

Figure 14 shows the temperature dependence AFM images of 50 alternating multilayer Si/Si+Sb thin films. As seen from the AFM images, the surface gets smoother with increasing temperatures from being unannealed to 200℃. The more temperature increment studies could be performed to see the effects in more detail since the surface is getting smoother when the temperature was increased two times. More detailed temperatures studies could show us more smoothing on the surfaces and more Sb material diffusing in the multilayer structures. To check the amount of diffusing Sb material in the multilayers, we are also planning to perform optical absorption spectroscopy.

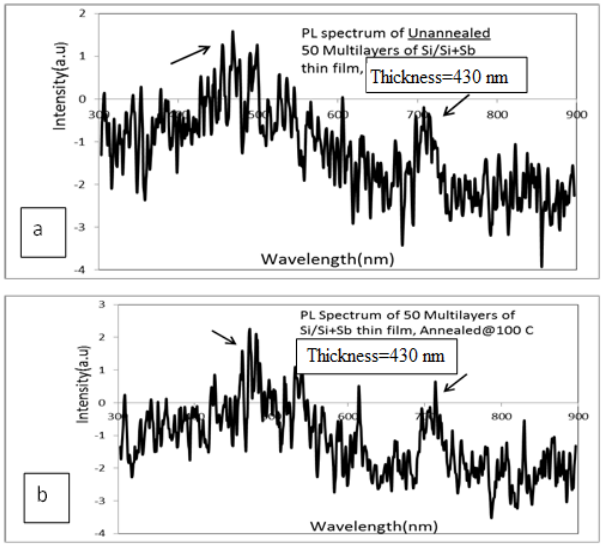

Figure 13. Photoluminescence Spectra of 50 alternating Si/Si+Sb multilayer thin films: a) Unannealed and b) annealed at 100℃

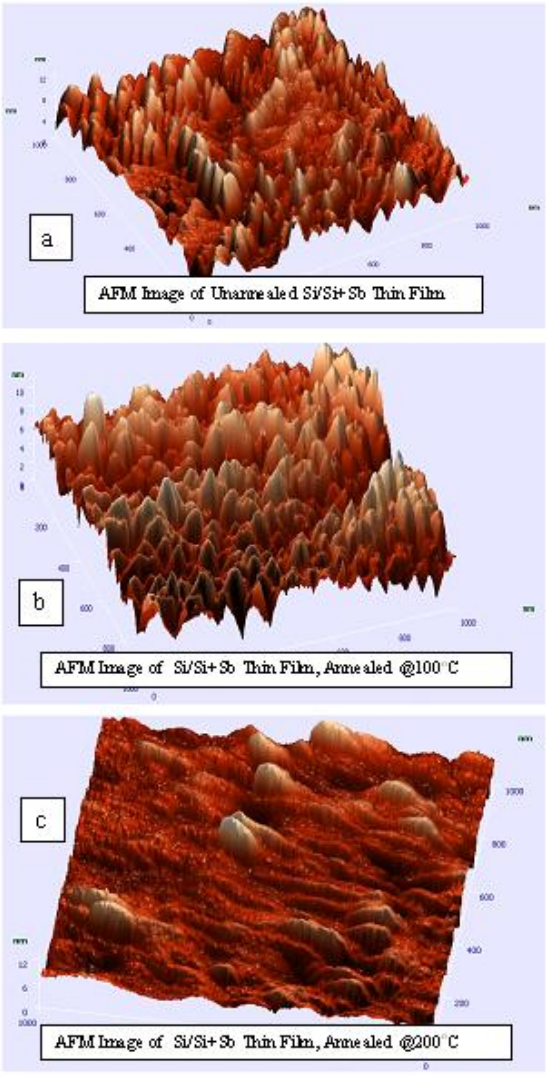

Figure 14. Temperature dependence AFM images of 50 alternating multilayer Si/Si+Sb thin films

4. Conclusions

Multilayer thin film systems from Si/Si+Sb have been deposited as 20 and 50 multilayer thermoelectric devices. The prepared thermoelectric devices were then introduced by high energy Si ions bombardment to form nano-dots and /or nano-clusters to tailor the thermoelectric and optical properties. Seebeck coefficient, van der Pauw resistivity measurements showed remarkable results at the suitable fluences as expected from the high efficient thermoelectric devices and materials. Transport properties addition to the van der Pauw resistivity like mobility, density, and Hall coefficient measurements showed shifting from n-type structure to p-type semiconductor structure. This might be arising from the charge carrier concentration due to high energy Si ion beam bombardment. AFM results show some smoothness on the surfaces depending on the annealing temperature. Further studies were planned in addition to the *thermal conductivity measurements* on S/Si+Sb thin film systems to reach more efficient thermoelectric devices.

ACKNOWLEDGEMENTS

Research sponsored by Materials Research Laboratory (MRL), National Science Foundation under NSF-EPSCOR R-II-3 Grant No. EPS-1158862, DOD under Nanotechnology Infrastructure Development for Education and Research through the Army Research Office # W911 NF-08-1-0425, and DOD Army Research Office # W911 NF-12-1-0063, U.S. Department of Energy National Nuclear Security Admin with grant# DE-NA0001896 and grant# DE-NA0002687, NSF-REU with Award#1156137.

REFERENCES

[1] Andreas Patyk, "Thermoelectric generators for efficiency improvement of power generation by motor generators – Environmental and economic perspectives", Applied Energy 102, 1448–1457 (2013).

[2] Ankam Bhaskar, Chia-Jyi Liu, J.J. Yuan, Ching-Lin Chang, "Thermoelectric properties of n-type $Ca_{1-x}Bi_xMn_{1-y}Si_yO_{3-d}$ (x = y = 0.00, 0.02, 0.03, 0.04, and 0.05) system", Journal of Alloys and Compounds 552, 236–239 (2013).

[3] Hee-Jung Lee, Hyun Sung Park, Seungwoo Han, Jung Yup Kim, "Thermoelectric properties of n-type Bi–Te thin films with deposition conditions using RF magnetron co-sputtering", Thermochimica Acta 542, 57– 61 (2012).

[4] Jiin-Yuh Jang, Ying-Chi Tsai, "Optimization of thermoelectric generator module spacing and spreader thickness used in a waste heat recovery system", Applied Thermal Engineering 51, 677-689 (2013).

[5] Ahmet Z. Sahin, Bekir S. Yilbas, "The thermoelement as thermoelectric power generator: Effect of leg geometry on the efficiency and power generation", Energy Conversion and Management 65, 26–32 (2013).

[6] Ping Fan, Ying-zhen Li, Zhuang-hao Zheng, Qing-yun Lin, Jing-ting Luo, Guang-xing Liang, Miao-qin Zhang, Min-cong Chen, "Thermoelectric properties optimization of Al-doped ZnO thin films prepared by reactive sputtering Zn–Al alloy target", Applied Surface Science 284, 145– 149 (2013).

[7] A. Hmood, A. Kadhim, H. Abu Hassan, "Fabrication and characterization of $Pb_{1-x}Yb_xTe$-based alloy thin-film thermoelectric generators grown by thermal evaporation technique", Materials Science in Semiconductor Processing 16, 612–618 (2013).

[8] Juncheng Guo, Xiuqin Zhang, Guozhen Su, Jincan Chen, "The performance analysis of a micro-/ nanoscaled quantum heat engine", Physica A 391, 6432–6439 (2012).

[9] I.P. Jain, Garima Agarwal, "Ion beam induced surface and interface engineering", Surface Science Reports 66, 77–172 (2011).

[10] S. Budak, R. Parker, C. Smith, C. Muntele, K. Heidary, R. B. Johnson, D.ILA, "Superlattice Multi-nanolayered Thin Films of SiO_2/SiO_2+Ge for Thermoelectric Device Applications", Journal of Intelligent Material Systems and Structures 24(11), 1357-1364 (2013).

[11] S. Budak, C. Smith, M. Pugh, K. Heidary, T. Colon, R.B. Johnson, D.ila, "MeV Si Ions Bombardment Effects on Thermoelectric Properties of Thermoelectric of SiO_2/SiO_2+Ge Nanolayers", Radiation Physics and Chemistry 81, 410-413 (2012).

[12] M. Pugh, S. Budak, C. Smith, J. Chacha, K. Ogbara, K. Heidary, R. B. Johnson, C. Muntele, D.ILA, "Fabrication and Characterization of Thermoelectric Generator from Si/Si+Ge multi-layer superlattice Nanolayered Films Effected by MeV Si Ions Bombardment", Mater. Res. Soc. Symp. Proc. Vol. 1267 © 2010 Materials Research Society 1267-DD05-14.

[13] S. Budak, S. Guner, C. Smith, R. A. Minamisawa, B. Zheng, C. Muntele, D. Ila, "Surface modification of Si/Ge multi-layers by MeV Si ion bombardment", Surface and Coating Technology 203, 2418-2421 (2009).

[14] C. Smith, M. Pugh, H. Martin, R. Hill, B. James, S. Budak, K. Heidary, C. Muntele, D. ILA, " Thermoelectric Generators of Sequentially Deposited Si/Si+Ge Nano-layered Superlattices", Mater. Res. Soc. Symp. Proc. Vol. 1181 © 2009 Materials Research Society, 1181-DD02-04.

[15] S. Budak, S. Guner, T. Hill, M. Black, S. B. Judah, C. Muntele, and D. Ila, "Fabrication and Characterization of Thermoelectric Generators From SiGe Thin Films", Mater. Res. Soc. Symp. Proc. Vol. 1102E © 2008 Materials Research Society 1102-LL05-03.

[16] B. Zheng, S. Budak, R. L. Zimmerman, C. Muntele, B. Chhay and D. ILA, "Effect of Layer Thickness on Thermoelectric Properties of Multilayered $Si_{1-x}Ge_x$/Si after Bombardment by 5MeV Si Ions", Surface and Coating Technology 201, 8531-8533 (2007).

[17] J. Chacha, S. Budak, C. Smith, D. McElhaney, M. Pugh, K. Ogbara, K. Heidary, R. B. Johnson, C. Muntele, D. Ila, "Thermoelectric Properties Of SiO_2/SiO_2+Au Nano-Layered Superlattices Modified By MeV Si Ions Beam," AIP Conf. Proc. 1336, 257-259 (2011).

[18] J. F. Ziegler, J. P. Biersack, U. Littmark, "The Stopping Range of Ions in solids," (Pergamon Press, Newyork, 1985).

[19] W. K. Chu, J. W. Mayer, M. -A. Nicolet, "Backscattering Spectrometry," (Academic Press, New York, 1978).

[20] X. Song, P. H. M. Botther, O. B. Karlsen, T. G. Finstad, and J. Tafto, "Impurity band conduction in the thermoelectric material ZnSb", Phys. Scr. T148, 014001 9(6pp) (2012).

[21] Jiasong Zhong, Xin Ma, Hongwei Lu, Xin Wang, Suling Zhang, Weidong Xiang, "Preparation and optical properties of sodium borosilicate glasses containing Sb nanoparticles", Journal of Alloys and Compounds 607, 177–182 (2014).

[22] Dean A. Eckhoff, Jason D. B. Sutin, Robert M. Clegg, and Enrico Gratton, Elena V. Rogozhina and Paul V. Braun, "Optical Characterization of Ultrasmall Si Nanoparticles Prepared through Electrochemical Dispersion of Bulk Si", J. Phys. Chem. B 109, 19786 -19797 (2005).

[23] L. B. Ma, A. L. Ji, C. Liu, Y. Q. Wang, and Z. X. Cao, "Low temperature growth of amorphous Si nanoparticles in oxide matrix for efficient visible photoluminescence", J. Vac. Sci. Technol. B 22(6), 2654-2657 (2004).

[24] F. X. Xiu, Z. Yang, L. J. Mandalapu, D. T. Zhao, and J. L. Liua, "Photoluminescence study of Sb-doped *p*-type ZnO films by molecular-beam epitaxy", Applied Physics Letters 87, 252102 (2005).